

# Observation of charged $\kappa$ in $J/\psi \rightarrow K^*(892)^\mp K_S \pi^\pm, K^*(892)^\mp \rightarrow K_S \pi^\mp$ at BESII

25 August, 2010; Revised 2 February, 2011

M. Ablikim<sup>1</sup>, J. Z. Bai<sup>1</sup>, Y. Bai<sup>1</sup>, Y. Ban<sup>15</sup>, X. Cai<sup>1</sup>, H. F. Chen<sup>22</sup>, H. S. Chen<sup>1</sup>,  
 J. C. Chen<sup>1</sup>, Jin Chen<sup>1</sup>, Y. B. Chen<sup>1</sup>, Y. P. Chu<sup>1</sup>, Y. S. Dai<sup>24</sup>, Z. Y. Deng<sup>1</sup>,  
 S. X. Du<sup>1a</sup>, J. Fang<sup>1</sup>, C. D. Fu<sup>1</sup>, Y. N. Gao<sup>19</sup>, Y. T. Gu<sup>4</sup>, Z. J. Guo<sup>20b</sup>,  
 F. A. Harris<sup>20</sup>, K. L. He<sup>1</sup>, M. He<sup>16</sup>, Y. K. Heng<sup>1</sup>, H. M. Hu<sup>1</sup>, T. Hu<sup>1</sup>,  
 G. S. Huang<sup>1c</sup>, X. T. Huang<sup>16</sup>, M. Ishida<sup>11</sup>, S. Ishida<sup>14</sup>, Y. P. Huang<sup>1</sup>, X. B. Ji<sup>1</sup>,  
 X. S. Jiang<sup>1</sup>, J. B. Jiao<sup>16</sup>, D. P. Jin<sup>1</sup>, S. Jin<sup>1</sup>, T. Komada<sup>14</sup>, S. Kurokawa<sup>8</sup>, G. Li<sup>1</sup>,  
 H. B. Li<sup>1</sup>, J. Li<sup>1</sup>, L. Li<sup>1</sup>, R. Y. Li<sup>1</sup>, W. D. Li<sup>1</sup>, W. G. Li<sup>1</sup>, X. L. Li<sup>16</sup>, X. N. Li<sup>1</sup>,  
 X. Q. Li<sup>13</sup>, Y. F. Liang<sup>17</sup>, B. J. Liu<sup>1d</sup>, C. X. Liu<sup>1</sup>, Fang Liu<sup>1</sup>, Feng Liu<sup>6</sup>,  
 H. M. Liu<sup>1</sup>, J. P. Liu<sup>23</sup>, H. B. Liu<sup>4e</sup>, Q. Liu<sup>20</sup>, R. G. Liu<sup>1</sup>, Z. A. Liu<sup>1</sup>, F. Lu<sup>1</sup>,  
 G. R. Lu<sup>5</sup>, J. G. Lu<sup>1</sup>, C. L. Luo<sup>12</sup>, F. C. Ma<sup>10</sup>, H. L. Ma<sup>1</sup>, Q. M. Ma<sup>1</sup>,  
 T. Maeda<sup>14</sup>, Z. P. Mao<sup>1</sup>, T. Matsuda<sup>21</sup>, X. H. Mo<sup>1</sup>, J. Nie<sup>1</sup>, M. Oda<sup>9</sup>,  
 S. L. Olsen<sup>20f</sup>, R. G. Ping<sup>1</sup>, J. F. Qiu<sup>1</sup>, G. Rong<sup>1</sup>, X. D. Ruan<sup>4</sup>, L. Y. Shan<sup>1</sup>,  
 L. Shang<sup>1</sup>, C. P. Shen<sup>20</sup>, X. Y. Shen<sup>1</sup>, H. Y. Sheng<sup>1</sup>, H. S. Sun<sup>1</sup>, S. S. Sun<sup>1</sup>,  
 Y. Z. Sun<sup>1</sup>, Z. J. Sun<sup>1</sup>, K. Takamatsu<sup>8</sup>, X. Tang<sup>1</sup>, J. P. Tian<sup>19</sup>, Y. Toi<sup>21g</sup>,  
 T. Tsuru<sup>8</sup>, K. Ukai<sup>8</sup>, G. S. Varner<sup>20</sup>, X. Wan<sup>1</sup>, L. Wang<sup>1</sup>, L. L. Wang<sup>1</sup>,  
 L. S. Wang<sup>1</sup>, P. Wang<sup>1</sup>, P. L. Wang<sup>1</sup>, Y. F. Wang<sup>1</sup>, Z. Wang<sup>1</sup>, Z. Y. Wang<sup>1</sup>,  
 C. L. Wei<sup>1</sup>, D. H. Wei<sup>3</sup>, N. Wu<sup>1</sup>, G. F. Xu<sup>1</sup>, X. P. Xu<sup>6</sup>, Y. Xu<sup>13</sup>, K. Yamada<sup>14</sup>,  
 I. Yamauchi<sup>18</sup>, M. L. Yan<sup>22</sup>, H. X. Yang<sup>1</sup>, M. Yang<sup>1</sup>, Y. X. Yang<sup>3</sup>, M. H. Ye<sup>2</sup>,  
 Y. X. Ye<sup>22</sup>, C. X. Yu<sup>13</sup>, C. Z. Yuan<sup>1</sup>, Y. Yuan<sup>1</sup>, Y. Zeng<sup>7</sup>, B. X. Zhang<sup>1</sup>,  
 B. Y. Zhang<sup>1</sup>, C. C. Zhang<sup>1</sup>, D. H. Zhang<sup>1</sup>, H. Q. Zhang<sup>1</sup>, H. Y. Zhang<sup>1</sup>,  
 J. W. Zhang<sup>1</sup>, J. Y. Zhang<sup>1</sup>, X. Y. Zhang<sup>16</sup>, Y. Y. Zhang<sup>17</sup>, Z. P. Zhang<sup>22</sup>,  
 J. W. Zhao<sup>1</sup>, M. G. Zhao<sup>13</sup>, P. P. Zhao<sup>1</sup>, Z. G. Zhao<sup>22</sup>, B. Zheng<sup>1</sup>, H. Q. Zheng<sup>15</sup>,  
 J. P. Zheng<sup>1</sup>, Z. P. Zheng<sup>1</sup>, B. Zhong<sup>12</sup>, L. Zhou<sup>1</sup>, K. J. Zhu<sup>1</sup>, Q. M. Zhu<sup>1</sup>,  
 X. W. Zhu<sup>1</sup>, Y. S. Zhu<sup>1</sup>, Z. A. Zhu<sup>1</sup>, B. S. Zou<sup>1</sup>  
 (BES Collaboration)

<sup>1</sup> *Institute of High Energy Physics, Beijing 100049, People's Republic of China*

<sup>2</sup> *China Center for Advanced Science and Technology (CCAST), Beijing 100080, People's Republic of China*

<sup>3</sup> *Guangxi Normal University, Guilin 541004, People's Republic of China*

<sup>4</sup> *Guangxi University, Nanning 530004, People's Republic of China*

<sup>5</sup> *Henan Normal University, Xinxiang 453002, People's Republic of China*

<sup>6</sup> *Huazhong Normal University, Wuhan 430079, People's Republic of China*

<sup>7</sup> *Hunan University, Changsha 410082, People's Republic of China*

<sup>8</sup> *KEK, High Energy Accelerator Research Organization, Ibaraki 305-0801, Japan*

<sup>9</sup> *Kokushikan University, Tokyo 154-8515, Japan*

<sup>10</sup> *Liaoning University, Shenyang 110036, People's Republic of China*

<sup>11</sup> *Meisei University, Tokyo 191-8506, Japan*

<sup>12</sup> *Nanjing Normal University, Nanjing 210097, People's Republic of China*

<sup>13</sup> *Nankai University, Tianjin 300071, People's Republic of China*

- <sup>14</sup> *Nihon University, Chiba 274-8501, Japan*
- <sup>15</sup> *Peking University, Beijing 100871, People's Republic of China*
- <sup>16</sup> *Shandong University, Jinan 250100, People's Republic of China*
- <sup>17</sup> *Sichuan University, Chengdu 610064, People's Republic of China*
- <sup>18</sup> *Tokyo Metropolitan College of Industrial Technology, Tokyo 140-0011, Japan*
- <sup>19</sup> *Tsinghua University, Beijing 100084, People's Republic of China*
- <sup>20</sup> *University of Hawaii, Honolulu, HI 96822, USA*
- <sup>21</sup> *University of Miyazaki, Miyazaki 889-2192, Japan*
- <sup>22</sup> *University of Science and Technology of China, Hefei 230026, People's Republic of China*
- <sup>23</sup> *Wuhan University, Wuhan 430072, People's Republic of China*
- <sup>24</sup> *Zhejiang University, Hangzhou 310028, People's Republic of China*
- <sup>a</sup> *Currently at: Zhengzhou University, Zhengzhou 450001, People's Republic of China*
- <sup>b</sup> *Currently at: Johns Hopkins University, Baltimore, MD 21218, USA*
- <sup>c</sup> *Currently at: University of Oklahoma, Norman, OK 73019, USA*
- <sup>d</sup> *Currently at: University of Hong Kong, Pok Fu Lam Road, Hong Kong*
- <sup>e</sup> *Currently at: Graduate University of Chinese Academy of Sciences, Beijing 100049, People's Republic of China*
- <sup>f</sup> *Currently at: Seoul National University, Seoul, 151-747, Republic of Korea*
- <sup>g</sup> *Currently at: Medipolis Medical Research Institute, Kagoshima 891-0304, Japan*

## Abstract

Using 58 million  $J/\psi$  decays obtained by BESII, a charged  $\kappa$  particle is observed in the analysis of the  $K_S\pi^\pm$  system recoiling against  $K^*(892)^\mp$  selected in  $J/\psi \rightarrow K_S K_S \pi^+ \pi^-$ . The mass and width values of the charged  $\kappa$  are obtained to be  $(826 \pm 49_{-34}^{+49})$  MeV/ $c^2$  and  $(449 \pm 156_{-81}^{+144})$  MeV/ $c^2$  for the Breit-Wigner parameters, and the pole position is determined to be  $(764 \pm 63_{-54}^{+71}) - i(306 \pm 149_{-85}^{+143})$  MeV/ $c^2$ . They are in good agreement with those of the neutral  $\kappa$  observed by the BES Collaboration.

*Key words:* Charged  $\kappa$ , low mass scalar,  $J/\psi$  decays,  $K^*(892)K\pi$

The experimental evidence on the existence of the low mass scalars below 1 GeV/ $c^2$ ,  $f_0(600)/\sigma$  and  $K_0^*(800)/\kappa$  particles [1], have stimulated studies on the lower mass meson structures. They may be classified in a possible  $\sigma$  nonet. However their nature is still controversial. The neutral  $\kappa$  particle was observed [2,3,4,5,6,7,8,9,10,11,12] in the analyses of  $K\pi$  scattering data. It has also been confirmed in the production processes,  $D^+$  decay into  $K^-\pi^+\pi^+$  by E791 at Fermilab [13], and  $J/\psi$  decay into  $\bar{K}^*(892)^0 K^+\pi^-$  by BESII [14]. The existence of a coherent  $K\pi$   $S$ -wave contribution was presented by FOCUS [15] in the analysis of semileptonic  $D$  decay,  $D^+ \rightarrow K^-\pi^+\mu^+\nu$ . Recently the necessity

of the  $\kappa$  was confirmed in the Dalitz plot analysis of the hadronic  $D$  decay,  $D^+ \rightarrow K^- \pi^+ \pi^+$  also by FOCUS [16] and later in the alternate analysis on the same data [17]. The CLEO Collaboration also confirmed the neutral  $\kappa$  in the same channel [18]. We may expect the existence of a charged  $\kappa$  according with isospin symmetry.

As for the charged  $\kappa$ , CLEO reported [19] the necessity of a  $S$ -wave  $K^\pm \pi^0$  resonance in the analysis of the interfering  $K^*(892)^+ K^-$  and  $K^*(892)^- K^+$  amplitudes in the decay,  $D^0 \rightarrow K^+ K^- \pi^0$ . Recently Belle [20] and BaBar [21] reported the necessity of the charged  $\kappa$  in the analyses of the  $K_S \pi^-$  mass distribution in the semileptonic  $\tau$  decay,  $\tau^- \rightarrow K_S \pi^- \nu_\tau$ . BaBar reported, however, no need for the charged  $\kappa$  in their analysis of the  $D$  decay into  $K^+ K^- \pi^0$  [22]. BES reported recently the charged  $\kappa$  in the partial wave analysis (PWA) of the combined system,  $K^*(892)^\mp K^\pm \pi^0$  and  $K^*(892)^\mp K_S \pi^\pm$ , in the decay,  $J/\psi \rightarrow K^\pm K_S \pi^\mp \pi^0$  [23]. The results for its resonance parameters are consistent with those of the neutral  $\kappa$  [14].

In this report, we present the results of a PWA of the  $K^*(892)^\mp K_S \pi^\pm$  system in the decay  $J/\psi \rightarrow K^*(892)^\mp K_S \pi^\pm$ ,  $K^*(892)^\mp \rightarrow K_S \pi^\mp$ , based on 58 million  $J/\psi$  decays collected by BESII at BEPC (Beijing Electron Positron Collider). The BESII detector is described in detail elsewhere [24]. The resonance parameters of the charged  $\kappa$  are obtained. In the PWA, a Breit-Wigner parameterization with an  $s$ -dependent width is used, and parameters for its pole position are determined. A different parameterization with a constant width is also examined. A branching ratio for  $J/\psi \rightarrow K^*(892)^\mp \kappa^\pm$  is determined.

In the event selection, the following requirements are imposed. The event must have six charged tracks with zero net charge. Each charged track must have a good helix fit in the main drift chamber (MDC) and satisfy for the polar angle  $\theta$ ,  $|\cos \theta| < 0.8$  and for the transverse momentum  $P_t$ ,  $P_t > 50 \text{ MeV}/c^2$  in the MDC. Two  $K_S \rightarrow \pi^+ \pi^-$  candidates,  $(\pi^+ \pi^-)^{(1)}$  or  $(\pi^+ \pi^-)^{(2)}$ , having a minimum value for  $\delta m_{K_S}$ ,

$$\delta m_{K_S} \equiv \sqrt{(m_{\pi^+ \pi^-}^{(1)} - m_{K_S})^2 + (m_{\pi^+ \pi^-}^{(2)} - m_{K_S})^2}, \quad (1)$$

where  $m_{\pi^+ \pi^-}^{(i)}$  ( $i = 1$  or  $2$ ) is the invariant mass of the  $(\pi^+ \pi^-)^{(i)}$  pair, are selected, and  $\delta m_{K_S}$  is required to satisfy  $\delta m_{K_S} \leq 0.02 \text{ GeV}/c^2$ . The surviving events are fitted kinematically under the hypothesis,  $J/\psi \rightarrow 3(\pi^+ \pi^-)$  and are required to have  $\chi^2$  value less than 15,  $\chi_{6\pi}^2 < 15$ . The positions of closest approach to the beam axis of the two pions of each  $(\pi^+ \pi^-)^{(i)}$  pair must agree within 0.05 m along the  $z$  axis (the electron beam direction).

The scatter plot of  $m_{\pi^+ \pi^-}^{(1)}$  versus  $m_{\pi^+ \pi^-}^{(2)}$  and its projected spectra for  $m_{\pi^+ \pi^-}^{(1)}$

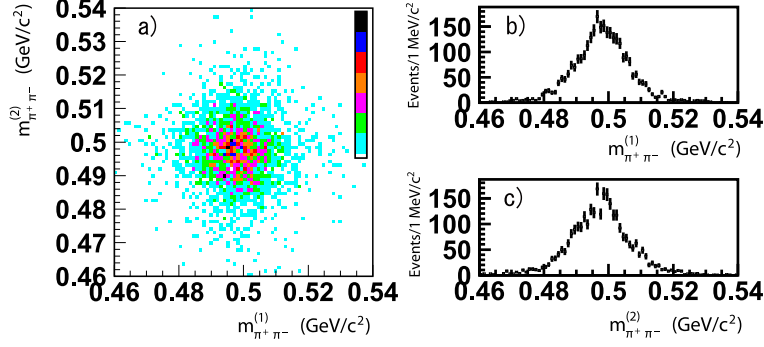


Fig. 1. Scatter plot for (a)  $m_{\pi^+\pi^-}^{(1)}$  versus  $m_{\pi^+\pi^-}^{(2)}$  and its projected spectra for (b)  $m_{\pi^+\pi^-}^{(1)}$  and (c)  $m_{\pi^+\pi^-}^{(2)}$ . The different colors on the color scale in (a) correspond to increments of two in the number of events in the bin.

and  $m_{\pi^+\pi^-}^{(2)}$  are shown in Fig. 1.

The selected  $m_{\pi^+\pi^-}^{(i)}$  event ( $i = 1$  or  $2$ ) is assigned to be  $K_S^{(i)}$  in the  $K_S K_S \pi^+ \pi^-$  events. After the selection, 2,933  $K_S K_S \pi^+ \pi^-$  events survive.

The scatter plots of the surviving events are displayed in Figs. 2a) and 2b) for the invariant mass of  $K_S^{(1)} \pi^+$ ,  $m_{K_S^{(1)} \pi^+}$  versus that of  $K_S^{(2)} \pi^-$ ,  $m_{K_S^{(2)} \pi^-}$  and for those of the alternate combinations,  $m_{K_S^{(2)} \pi^+}$  versus  $m_{K_S^{(1)} \pi^-}$ , respectively. The projected spectra are shown for  $K_S^{(1)} \pi^+$  (Fig. 2c)) and  $K_S^{(2)} \pi^-$  (Fig. 2d)), and for those of alternate combinations,  $K_S^{(2)} \pi^+$  (Fig. 2e)) and  $K_S^{(1)} \pi^-$  (Fig. 2f)). Their sum spectrum is also shown in Fig. 2g). Concentrations of events coming from  $K^*(892)^\pm$  are seen in the spectra. The scatter plot for the invariant mass of  $K_S K_S$  versus that of  $\pi^+ \pi^-$  is shown with its projected spectra in Fig. 3. A  $\rho(770)$  peak is also seen in the  $\pi^+ \pi^-$  spectrum.

Before the event selection of  $K^*(892)^\mp K_S \pi^\pm$  for the PWA, other possible backgrounds are studied. Selection efficiencies are determined by Monte Carlo simulation for the decays,  $J/\psi \rightarrow 3(\pi^+ \pi^-)$ ,  $J/\psi \rightarrow K^+ K_S \pi^- \pi^+ \pi^-$ ,  $J/\psi \rightarrow \gamma \eta_c$ ,  $\eta_c \rightarrow K_S K_S \pi^+ \pi^-$ ,  $J/\psi \rightarrow \gamma K_S K_S \pi^+ \pi^-$ ,  $J/\psi \rightarrow \gamma K^*(892)^\mp K^*(892)^\pm$ ,  $J/\psi \rightarrow \gamma K^*(892)^\mp K_S \pi^\pm$  and  $J/\psi \rightarrow \gamma 3(\pi^+ \pi^-)$  which could contribute background to the study of  $J/\psi \rightarrow K^*(892)^\mp K_S \pi^\pm \rightarrow K_S K_S \pi^+ \pi^-$ . Other decay modes such as  $J/\psi \rightarrow 3(\pi^+ \pi^-) \pi^0$  and  $J/\psi \rightarrow K_S K_S \pi^+ \pi^- \pi^0$  are also studied. The largest background is from  $J/\psi \rightarrow 3(\pi^+ \pi^-)$ . Those for  $J/\psi \rightarrow \gamma \eta_c$ ,  $\eta_c \rightarrow K_S K_S \pi^+ \pi^-$ ,  $J/\psi \rightarrow \gamma K_S K_S \pi^+ \pi^-$ ,  $J/\psi \rightarrow \gamma K^*(892) \bar{K}^*(892)$  and  $J/\psi \rightarrow \gamma K^*(892)^\pm K_S \pi^\mp$  are small. The last two processes which have  $K^*(892)$  ( $K^*(892)$  and  $\bar{K}^*(892)$ ) are suppressed and negligible. Others are also found to be negligible.

The contribution of background events from  $J/\psi \rightarrow 3(\pi^+ \pi^-)$  is checked using both the distributions of  $\delta m_{K_S}$  and the proper time,  $c\tau$  of  $K_S$ . The  $\delta m_{K_S}$  distribution of data shows an excess of events compared with  $K_S K_S \pi^+ \pi^-$

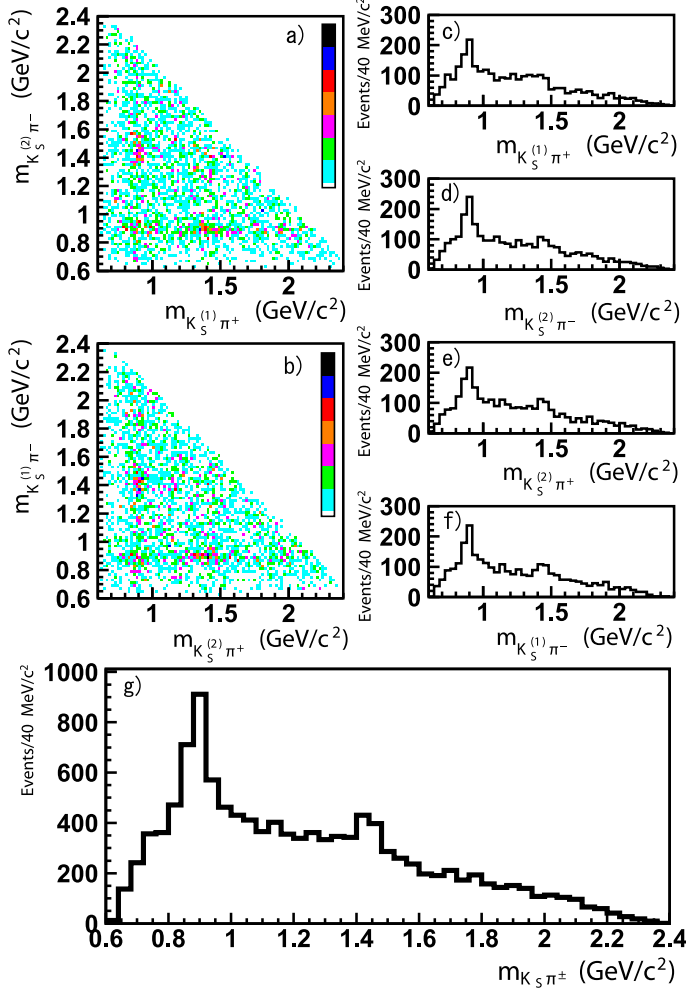


Fig. 2. Scatter plots for (a)  $m_{K_S^{(1)}\pi^+}$  versus  $m_{K_S^{(2)}\pi^-}$  and (b)  $m_{K_S^{(2)}\pi^+}$  versus  $m_{K_S^{(1)}\pi^-}$  and their projected spectra for (c)  $m_{K_S^{(1)}\pi^+}$ , (d)  $m_{K_S^{(2)}\pi^-}$ , (e)  $m_{K_S^{(2)}\pi^+}$ , (f)  $m_{K_S^{(1)}\pi^-}$  and (g) their sum,  $m_{K_S\pi^\pm}$ . The different colors on the color scale in (a) and (b) correspond to increment of one in the number of event in the bin.

Monte Carlo simulation outside the selection region,  $\delta m_{K_S} > 20 \text{ MeV}/c^2$ . Fitting the excess with parameters obtained for  $3(\pi^+\pi^-)$  by Monte Carlo simulation and extrapolating the fit down into the selection region gives a contribution from  $3(\pi^+\pi^-)$  to be  $(8.7 \pm 0.1)\%$ . Next, the  $c\tau$  distribution is studied. There is an excess of events for  $c\tau$  less than 1 cm compared with what is expected from Monte Carlo simulation of  $K_S K_S \pi^+ \pi^-$  events. The excess events are assumed to be  $3(\pi^+\pi^-)$ , and their amount is estimated to be  $(11.9 \pm 0.8)\%$  of the total  $K_S$  events. Though the two values differ, they give an indication of the amount of background from the  $3(\pi^+\pi^-)$  events. In the PWA,  $K^*(892)$  side-band events are used for the background estimation, and they may include not only those from  $3(\pi^+\pi^-)$  but also from other processes, as described below.

Four combinations of  $K_S^{(i=1 \text{ or } 2)}\pi^{(+ \text{ or } -)}$  events recoiling against  $K^*(892)^{(- \text{ or } +)}$

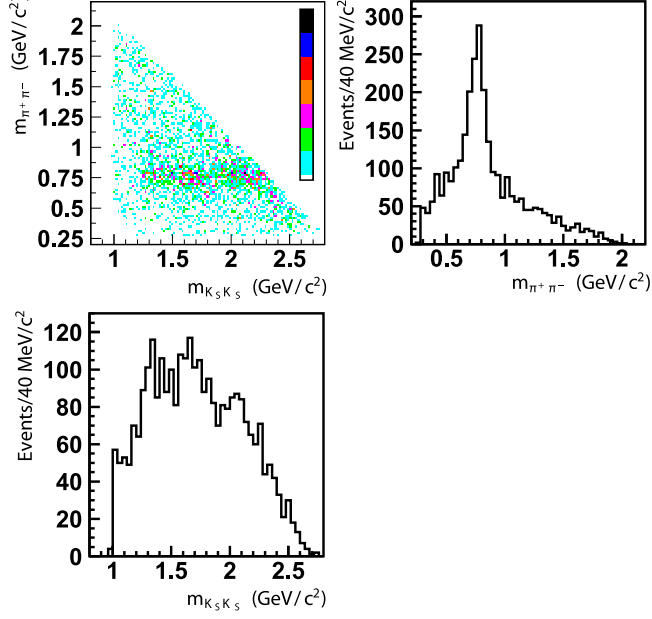


Fig. 3. Scatter plot for  $m_{K_S K_S}$  versus  $m_{\pi^+\pi^-}$  and its projected spectra for  $m_{K_S K_S}$  and  $m_{\pi^+\pi^-}$ . The different colors on the color scale in the scatter plot correspond to increment of one in the number of event in the bin.

are selected in  $J/\psi \rightarrow K_S^* K_S \pi^+ \pi^-$  for the PWA. Preceding the selection, background events associated with  $\rho(770)^0$  are rejected with the condition,  $|m_{\pi^+\pi^-} - 775| > 100 \text{ MeV}/c^2$ . The conditions for  $K^*(892)$  selection and background rejection of alternate combination channels in the four combinations are as follows;

- (1)  $J/\psi \rightarrow K^*(892)^- K_S^{(1)} \pi^+$  :  $|m_{K_S^{(2)} \pi^-} - 892| < 80 \text{ MeV}/c^2$ ,  
 $|m_{K_S^{(1)} \pi^-} - 892| > 40 \text{ MeV}/c^2$ ,  $|m_{K_S^{(2)} \pi^+} - 892| > 40 \text{ MeV}/c^2$ ,
  - (2)  $J/\psi \rightarrow K^*(892)^+ K_S^{(2)} \pi^-$  :  $|m_{K_S^{(1)} \pi^+} - 892| < 80 \text{ MeV}/c^2$ ,  
 $|m_{K_S^{(2)} \pi^+} - 892| > 40 \text{ MeV}/c^2$ ,  $|m_{K_S^{(1)} \pi^-} - 892| > 40 \text{ MeV}/c^2$ ,
  - (3)  $J/\psi \rightarrow K^*(892)^- K_S^{(2)} \pi^+$  :  $|m_{K_S^{(1)} \pi^-} - 892| < 80 \text{ MeV}/c^2$ ,  
 $|m_{K_S^{(2)} \pi^-} - 892| > 40 \text{ MeV}/c^2$ ,  $|m_{K_S^{(1)} \pi^+} - 892| > 40 \text{ MeV}/c^2$ ,
- or
- (4)  $J/\psi \rightarrow K^*(892)^+ K_S^{(1)} \pi^-$  :  $|m_{K_S^{(2)} \pi^+} - 892| < 80 \text{ MeV}/c^2$ ,  
 $|m_{K_S^{(1)} \pi^+} - 892| > 40 \text{ MeV}/c^2$ ,  $|m_{K_S^{(2)} \pi^-} - 892| > 40 \text{ MeV}/c^2$ .

After selection, 1,338 events survive for the sum of the four channels and are used in the PWA.

The  $m_{K_S \pi}$  distributions are shown for the four  $K^*(892)^\mp K_S \pi^\pm$  combinations in Figs. 4a)- 4d) and for their sum in Fig. 4e). Clear peaks around  $900 \text{ MeV}/c^2$  and around  $1400 \text{ MeV}/c^2$  are observed in the sum distribution. The  $m_{K^* \mp \pi^\pm}$  distributions are shown in Fig. 5. No distinct structure is seen in the figures.  $K_1(1270)$  which preferentially decays into  $\rho K_S$  as a background is reduced.

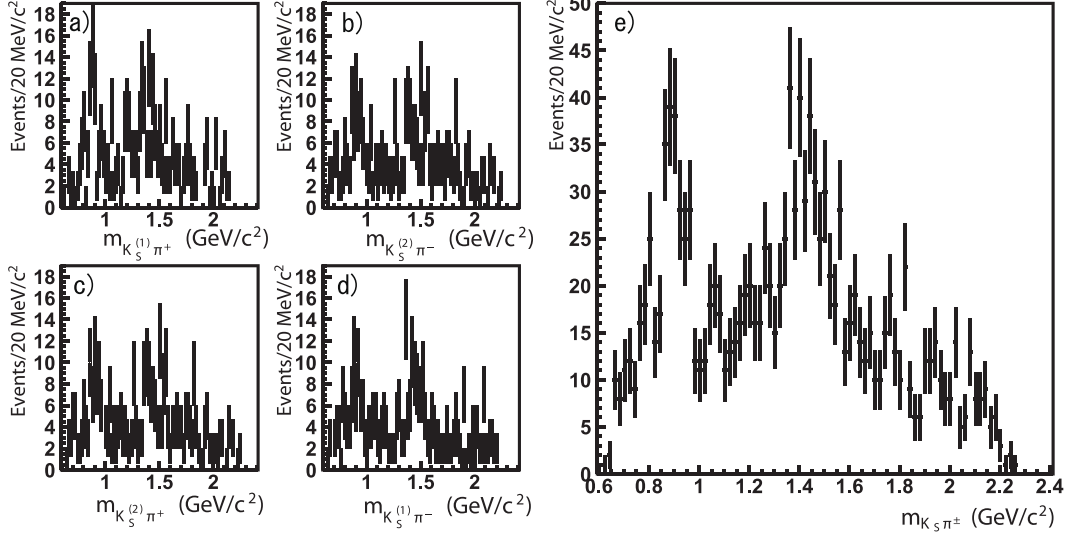


Fig. 4.  $m_{K_S\pi^\pm}$  distributions for (a)  $m_{K_S^{(1)}\pi^+}$ , (b)  $m_{K_S^{(2)}\pi^-}$ , (c)  $m_{K_S^{(2)}\pi^+}$  and (d)  $m_{K_S^{(1)}\pi^-}$  and (e) their sum,  $m_{K_S\pi^\pm}$ .

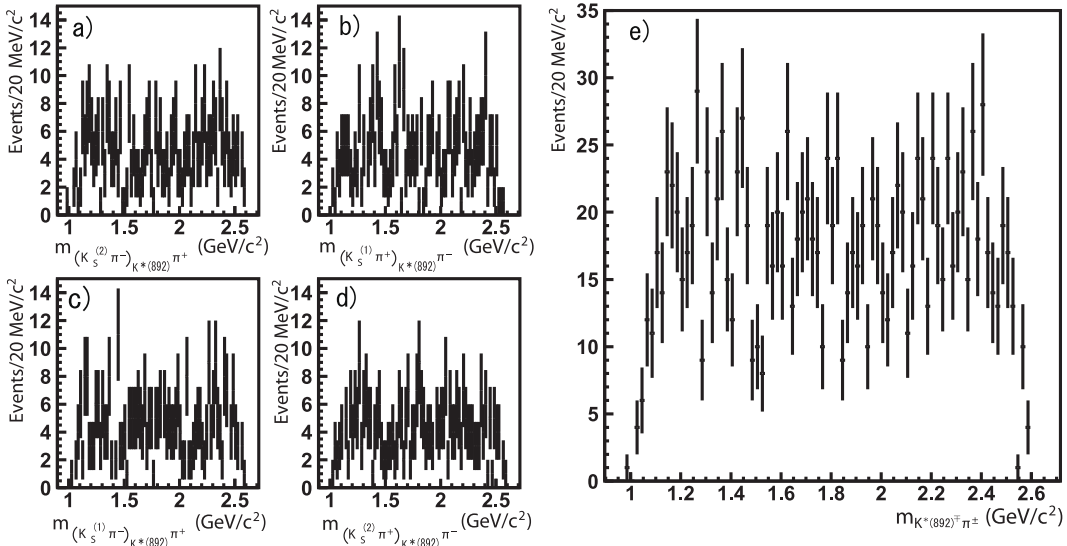


Fig. 5.  $m_{K^*(892)^\mp\pi^\pm}$  distributions for (a)  $m_{(K_S^{(2)}\pi^-)_{K^*(892)\pi^+}}$ , (b)  $m_{(K_S^{(1)}\pi^+)_{K^*(892)\pi^-}}$ , (c)  $m_{(K_S^{(1)}\pi^-)_{K^*(892)\pi^+}}$ , (d)  $m_{(K_S^{(2)}\pi^+)_{K^*(892)\pi^-}}$  and (e) their sum,  $m_{K^*(892)^\mp\pi^\pm}$ .

The Dalitz plot of the summed events is shown for  $K_S\pi^\pm$  and  $K^*(892)^\mp\pi^\pm$  in Fig. 6. Two vertical bands correspond to the peak around 892 MeV/c<sup>2</sup> and around 1430 MeV/c<sup>2</sup>.

The  $m_{K_S\pi^\pm}$  distribution of the  $K^*(892)^\mp$  side-band events selected in the region,  $80 \text{ MeV}/c^2 < |M_{K^*(892)} - 892| < 160 \text{ MeV}/c^2$  is shown in Fig. 7. The  $m_{K_S\pi^\pm}$  distribution after the final selection but without the  $K^*(892)$  requirement is inserted in the figure. The side band selection regions are indicated by the hatched area. The following processes,  $K^*(892)K_0^*(1430)$ ,  $K^*(892)K_2^*(1430)$ ,

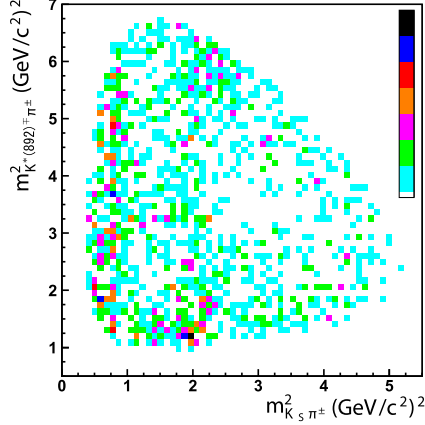


Fig. 6. Dalitz plot of  $K_S\pi^\pm$  versus  $K^*(892)^\mp\pi^\pm$ . The different colors on the color scale correspond to increment of one in the number of event in the bin.

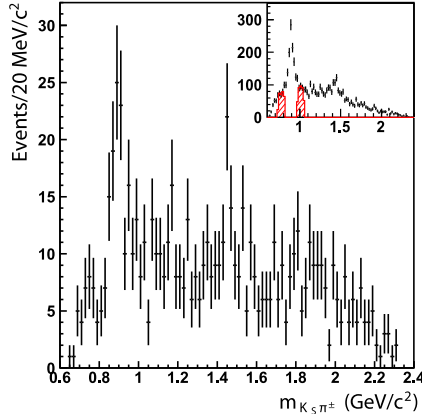


Fig. 7.  $m_{K_S\pi^\pm}$  distribution of  $K^*(892)^\mp$  side-band events. Insertion:  $m_{K_S\pi^\pm}$  distribution after final selection except the  $K^*(892)$  requirement. The hatched areas (red color) show the region for the side-band selection.

$K_0^*(1430)K_0^*(1430)$ ,  $K_0^*(1430)\kappa$ ,  $K_1(1270)K_S$ ,  $K_1(1400)K_S$  and  $K^*(892)K_S\pi$  from alternate combination channels and a background process,  $3(\pi^+\pi^-)$ , contribute to the side band events.

The contribution from a non-interfering phase space-like background is estimated from the  $K^*(892)^\mp$  side-band events in the  $K_S\pi^\pm$  mass region between  $1.6 \text{ GeV}/c^2$  and  $2.0 \text{ GeV}/c^2$  where these events are assumed to dominate. Uncertainties for the estimation of this contribution will be considered in the PWA and taken into the estimation for the systematic errors of the  $\kappa$  parameters.

The variant mass and width method (VMW method) [25] is used for the analysis. The VMW method is a covariant field-theoretical approach consistent with generalized unitarity. In this method, the total amplitude is expressed as a coherent sum of respective amplitudes corresponding to the relevant processes of strong interactions among all color singlet hadrons. As the bases of S-matrix



for the strong interaction, all unstable/resonant as well as stable hadrons are to be included. The propagator of a resonant particle is given by the conventional Feynman propagator with substitution of  $i\epsilon$  by  $i\sqrt{s}\Gamma(s)$ .

Four processes are considered, i) via  $K_S\pi^\pm$  resonances,  $J/\psi \rightarrow K^*(892)^\mp R_{K_S\pi^\pm}$ , ii) via  $K^*(892)^\mp\pi^\pm$  resonances,  $J/\psi \rightarrow K_S R_{K^*(892)^\mp\pi^\pm}$ , iii) via  $K^*(892)^\mp K_S$  resonances,  $J/\psi \rightarrow \pi^\pm R_{K^*(892)^\mp K_S}$ , and iv) via a direct  $K^*(892)^\mp K_S\pi^\pm$  decay, where  $R_{K_S\pi^\pm}$ ,  $R_{K^*(892)^\mp\pi^\pm}$  and  $R_{K^*(892)^\mp K_S}$  stand for the intermediate resonant states decaying into  $K_S\pi$  ( $\kappa$ ,  $K_0^*(1430)$ ,  $K_2^*(1430)$ ,  $K_2^*(1980)$ ),  $K^*(892)^\mp\pi$  ( $K_1(1270)$ ,  $K_1(1400)$ ), and  $K^*(892)^\mp K_S$  ( $b_1(1235)$ ), respectively.

For the scalar  $K_S\pi$  resonant states,  $\kappa$  and  $K_0^*(1430)$  are considered for  $R_{K_S\pi^\pm}$ . The Lagrangian of strong interaction,  $\mathcal{L}_S$  describing the process is taken to be the most simple form. The Lagrangian,  $\mathcal{L}_S$  and corresponding amplitude,  $\mathcal{F}_S$  are given as follows,

$$\begin{aligned}\mathcal{L}_S &= \sum_{R=\kappa, K_0^*} (\xi_R \psi_\mu K_\mu^* R + g_R R K_S \pi), \\ \mathcal{F}_S &= S_{h_\psi h_{K^*}} \sum_{R=\kappa, K_0^*} r_R e^{i\theta_R} \Delta_R(s_{K_S\pi}), \\ \Delta_R(s_{K_S\pi}) &= \frac{m_R \Gamma_R}{m_R^2 - s_{K_S\pi} - i\sqrt{s_{K_S\pi}} \Gamma_R(s_{K_S\pi})},\end{aligned}\tag{2}$$

where  $\Delta_R(s_{K_S\pi})$  is the Breit-Wigner formula with  $\Gamma_R(s_{K_S\pi}) = pg_R^2/(8\pi s_{K_S\pi})$ , describing the decay of  $R = \kappa$  and  $K_0^*(1430)$ , and  $S_{h_\psi h_{K^*}} \equiv \epsilon_\mu^{(h_\psi)} \tilde{\epsilon}_\mu^{(h_{K^*})}$  is a factor due to helicity combinations between relevant particles.  $p$  is a momentum of the pion decaying from the  $K_S\pi$  system at rest.  $S_{h_\psi h_{K^*}} r_R e^{i\theta_R}$  describes the S-matrix element,  ${}_{out}\langle RK^* | J/\psi \rangle_{in}$ , where  $e^{i\theta_R}$  parameterizes the rescattering phase of the outgoing wave,  ${}_{out}\langle RK^* |$ . This form of  $\mathcal{F}_S$  is consistent with the generalized unitarity of the S-matrix.

The decay amplitudes through  $R_{(K_S\pi)_D}$ ,  $R_{K^*(892)^\mp\pi}$  and  $R_{K^*(892)^\mp K}$  denoted as  $\mathcal{F}_D$ ,  $\mathcal{F}_{K_1}$ , and  $\mathcal{F}_{b_1}$ , respectively, are obtained in a similar manner. The direct  $K^*(892)K_S\pi$  production amplitude is taken to be  $\mathcal{F}_{direct} = S_{h_\psi h_{K^*}} r_{K_S\pi} e^{i\theta_{K_S\pi}}$ . The total amplitude,  $\mathcal{F}$  is given by the sum of all amplitudes,  $\mathcal{F} = \mathcal{F}_S + \mathcal{F}_D + \mathcal{F}_{K_1} + \mathcal{F}_{b_1} + \mathcal{F}_{direct}$ . Details of the amplitudes considered in the analysis are described in [26].

Background events of  $K^*(892)_{BG}$  decaying into  $K_S\pi$  are taken into the analysis. They are events of  $K^*(892)$  recoiling against  $K_S\pi$  systems. The  $K_S\pi$  system is in the mass region of  $K^*(892)$  in an alternate combination channel of the  $K^*(892)K_S\pi$ , and is seen at the cross region of the  $K^*(892)$  bands of the  $K_S\pi$  scatter plots in Fig. 2a) or 2b). The process  $K^*(892)K^*(892)_{BG}$  is described by an amplitude being incoherent with  $\mathcal{F}$ . The non-interfering phase space-like background is also considered. Its amount estimated from

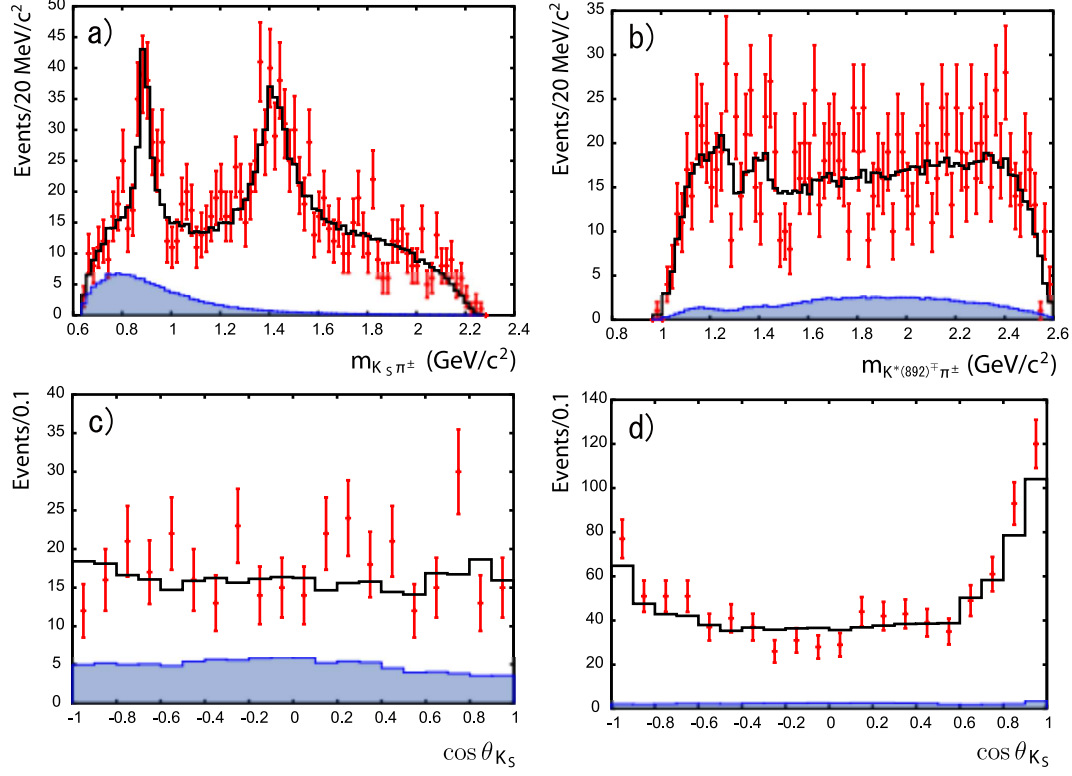


Fig. 8. Results of the analysis. The mass distributions of (a)  $K_S\pi^\pm$  and (b)  $K^*(892)^\mp\pi^\pm$  and the angular distributions of  $K_S$  in the  $K_S\pi$  center of mass system for the  $K_S\pi$  mass regions (c) below  $1 \text{ GeV}/c^2$  and (d) above  $1 \text{ GeV}/c^2$ . Crosses with error bars are the experimental data and solid histograms are fitted results. The shaded histograms (blue color) show the contributions from the charged  $\kappa$ .

the  $K^*(892)$  side-band events is fixed in the analysis.

The PWA is performed on the  $K_S\pi$  and the  $K^*(892)\pi$  mass distributions and the angular distributions of  $K_S$  in the  $K_S\pi$  center of mass system. The BES detector simulation code, SIMBES [27] which is a GEANT3-based Monte Carlo program is used for the acceptance correction.  $\chi^2$  fitting is utilized in the partial wave analysis. The MINUIT package of CERNLIB [28] is used for minimization of functions and estimation of uncertainties in the fitting. Fig. 8 shows the results of fitting on  $m_{K_S\pi^\pm}$ ,  $m_{K^*(892)^\mp\pi^\pm}$ , and the angular distributions of  $K_S$  in the  $K_S\pi$  center of mass system for the  $K_S\pi$  mass regions below and above  $1 \text{ GeV}/c^2$ . The  $K_S\pi$  mass distribution and the  $K_S$  angular distributions are well reproduced by the fit. The shaded histograms (blue color) show the contributions of the  $\kappa$  resonance.

The parameter values of mass and width of the resonances except the  $\kappa$  resonance are fixed in the PWA to those summarized in the PDG tables [1]. The uncertainties of  $1\sigma$  deviations of the resonance parameters are included in the estimation of the systematic errors of the  $\kappa$  parameters.

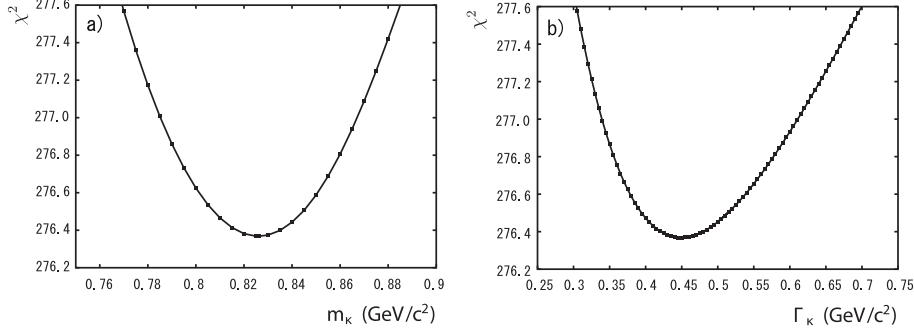


Fig. 9. Mass and width scan for the charged  $\kappa$ , a) mass scan and b) width scan.

Events around  $1.9 \text{ GeV}/c^2$  in the  $M_{K_S\pi}$  distribution require a resonance in the fitting. Resonances,  $K_0^*(1950)$  and  $K_2^*(1980)$ , are tried. The significance obtained for the  $K_2^*(1980)$  is better than that for  $K_0^*(1950)$  by  $1.43\sigma$ , and  $K_2^*(1980)$  is included in the PWA. The  $K^*(892)^\mp K_S\pi^\pm$  direct decay which interferes with  $\kappa$  and other resonances is found to have less than  $1\sigma$  significance and is not included in the present analysis.

Uncertainties of the contribution of the non-interfering phase space-like background are included in the estimation of the systematic errors of the  $\kappa$  parameters, assuming this background to be uncertain by  $\pm 30\%$ .

Breit-Wigner parameters for mass and width of the charged  $\kappa$  are obtained to be

$$m_\kappa = 826 \pm 49_{-34}^{+49} \text{ MeV}/c^2 \quad \text{and} \quad \Gamma_\kappa = 449 \pm 156_{-81}^{+144} \text{ MeV}/c^2,$$

where the first errors are statistical and the second ones are systematic. The pole position of the charged  $\kappa$  is determined to be

$$(764 \pm 63_{-54}^{+71}) - i(306 \pm 149_{-85}^{+143}) \text{ MeV}/c^2$$

from the Breit-Wigner parameters.

The  $\kappa$  resonance parameters are scanned and are confirmed to have no local minimum as shown in Fig. 9. The  $\chi^2$  value of the PWA including charged  $\kappa$  is 276 with 185 degrees of freedom (d.o.f). That without the charged  $\kappa$  is 344 with 189 d.o.f. This indicates the significance of the charged  $\kappa$  to be  $7.5\sigma$ .

The value for each distribution,  $\chi^2/N_{data}$  ( $N_{data}$ : number of data points) in the fit including the charged  $\kappa$  may help to give ideas on the fitting affairs of the PWA. They are 0.99 for  $\chi^2_{m_{K_S\pi}}/N_{data}$ , 1.82 for  $\chi^2_{m_{K^*\pi}}/N_{data}$ , 1.39 for  $\chi^2_{\cos\theta_{K_S}}(m_{K_S\pi} \leq 1 \text{ GeV}/c^2)/N_{data}$  and 1.09 for  $\chi^2_{\cos\theta_{K_S}}(m_{K_S\pi} > 1 \text{ GeV}/c^2)/N_{data}$ . These values show that the contribution to the total  $\chi^2$  comes mostly from the fit of the  $K^*\pi$  mass distribution.

The parameter values obtained for the charged  $\kappa$  are summarized in Table 1. The mass and width values for other resonances used in the PWA are also

Table 1

Observed values for parameters of the charged kappa and for phases of resonances. Mass and width values of resonances except  $\kappa$  are fixed to those in the PDG tables [1].

Process	Mass (MeV/ $c^2$ )	Width (MeV/ $c^2$ )	$\theta$ (Deg.)
$\kappa \rightarrow K\pi$	$826 \pm 49_{-34}^{+49}$	$449 \pm 156_{-81}^{+144}$	0 (fixed)
$K_0^*(1430) \rightarrow K\pi$	1425	270	37
$K_2^*(1430) \rightarrow K\pi$	1426	99	157
$K_2^*(1980) \rightarrow K\pi$	1973	373	16
$K_1(1270) \rightarrow K^*(892)\pi$	1272	90	111
$K_1(1400) \rightarrow K^*(892)\pi$	1403	174	111
$b_1(1235) \rightarrow K^*(892)K$	1230	142	235
$K^*(892)_{BG} \rightarrow K\pi$	892	51	—
Non-interfering phase space-like B.G.	—	—	—

Table 2

Numerical values of the relative contributions of the resonances and backgrounds. They are normalized by the total contribution. Uncertainties are statistical.

$J/\psi \rightarrow \kappa K^*(892)$	$0.109_{-0.021}^{+0.023}$
$J/\psi \rightarrow K_0^*(1430)K^*(892)$	$0.115_{-0.042}^{+0.052}$
$J/\psi \rightarrow K_2^*(1430)K^*(892)$	$0.114_{-0.033}^{+0.038}$
$J/\psi \rightarrow K_2^*(1980)K^*(892)$	$0.017_{-0.011}^{+0.018}$
$J/\psi \rightarrow K_1(1270)K$	$0.044_{-0.013}^{+0.015}$
$J/\psi \rightarrow K_1(1400)K$	$0.069_{-0.023}^{+0.028}$
$J/\psi \rightarrow b_1(1235)\pi$	$0.069_{-0.024}^{+0.030}$
$K^*(892)_{BG}$	$0.084_{-0.014}^{+0.015}$
Non-interfering phase space-like B.G.	$0.328 \pm 0.098$

shown. The relative phases obtained for resonances are in the last column. The parameter values obtained for the charged  $\kappa$  are in good agreement with those for the neutral  $\kappa$  [14],  $m_\kappa = (878 \pm 23_{-55}^{+64})$  MeV/ $c^2$  and  $\Gamma_\kappa = (499 \pm 52_{-87}^{+55})$  MeV/ $c^2$ .

Table 2 shows the relative contributions of the relevant resonances and of the backgrounds from  $K^*(892)_{BG}$  and the non-interfering phase space-like background. The relative contribution is obtained by integration of the amplitude squared of the relevant resonance or background with normalization by the

total contribution which is from a sum of the total amplitude squared and the background amplitudes squared.

A constant width parameterization of the Breit-Wigner formula for each resonance is also tried in the PWA. The mass and width values of  $\kappa$  are obtained to be  $m_\kappa = 656 \pm 119^{+56}_{-186}$  MeV/ $c^2$  and  $\Gamma_\kappa = 536 \pm 211^{+440}_{-144}$  MeV/ $c^2$ , and the parameters for the pole position are determined to be  $(702 \pm 113^{+54}_{-175}) - i(250 \pm 88^{+163}_{-62})$  MeV/ $c^2$ . They are consistent with those obtained for the s-dependent width in Eq. (2).

Recently the BES Collaboration reported [23] the mass and width for a charged  $\kappa$  in  $K_S\pi^\pm$  and  $K^\pm\pi^0$  recoiling against  $K^*(892)^\mp$  in  $J/\psi \rightarrow K^\pm K_S\pi^\mp\pi^0$  to be  $(884 \pm 40^{+11}_{-22})$  MeV/ $c^2$  and  $(478 \pm 77^{+71}_{-41})$  MeV/ $c^2$ , respectively. The parameter values of the  $\kappa$  resonance are in good agreement with those of the neutral  $\kappa$  [14] and also with those of the present results.

A possible contribution from  $K^*(892)^\pm$  recoiling against  $K^*(892)^\mp$  is studied. This process may proceed via one photon annihilation of the  $J/\psi$  decay. Including both  $K^*(892)^\pm$  and the background,  $K^*(892)^\pm_{BG}$ , the PWA is unable to determine their amplitudes separately due to the low statistics of the present data. Also the PWA with  $K^*(892)^\pm$  instead of  $K^*(892)^\pm_{BG}$  finds almost the same results for the mass, width, amplitude, and phase values of the  $\kappa$ ,  $K^*_0(1430)$ ,  $K^*_2(1430)$  and  $K^*_2(1980)$ , and slightly different results of  $K_1(1270)$ ,  $K_1(1400)$  and  $b_1(1235)$ . The resonance state,  $K^*(1410)^\pm$  is also examined in the PWA. The results for  $K^*(1410)^\pm$  are consistent with zero with little effect on the parameters of other resonances. The process,  $K^*(1410)$  recoiling against  $K^*(892)$  in the  $J/\psi$  decay is definitely suppressed.

The branching ratio for  $J/\psi \rightarrow K^*(892)^\mp\kappa^\pm$  is determined. The number of events for  $K^*(892)^\mp\kappa^\pm$  is determined to be  $142 \pm 28$  in the PWA, and the number of  $J/\psi$  events collected by BESII is  $(5.8 \pm 0.3) \times 10^7$ . The detection efficiency is estimated to be  $4.88 \times 10^{-3}$  by Monte Carlo simulation. It includes the detector efficiencies and isospin factors of the decays,  $K^0 \rightarrow K_S$  and  $K_S \rightarrow \pi^+\pi^-$ . The branching ratio for the process,  $BR(J/\psi \rightarrow K^*(892)^\mp\kappa^\pm)$  is determined to be

$$\begin{aligned} BR(J/\psi \rightarrow K^*(892)^\mp\kappa^\pm) &= \frac{142}{(5.8 \times 10^7)(4.88 \times 10^{-3})} \times \frac{9}{4} \\ &= (1.13 \pm 0.22^{+0.49}_{-0.22}) \times 10^{-3}, \end{aligned}$$

where the first error is statistical and the second systematic. The factor,  $\frac{9}{4}$  comes from the isospin weight for the decay modes of  $\kappa$  and  $K^*(892)$ . The systematic errors are estimated by square root of the sum of uncertainties for the number of  $K^*(892)^\mp\kappa^\pm$  events obtained in PWA, for the detection efficiency in Monte Carlo simulation, and for the number of  $J/\psi$  events. The

branching ratio is also reported by the BES Collaboration [23] in the analysis of  $J/\psi \rightarrow K^*(892)^\mp \kappa^\pm \rightarrow K^\mp K_S \pi^\pm \pi^0$  to be  $(1.09 \pm 0.18_{-0.54}^{+0.94}) \times 10^{-3}$ , which is consistent with the present result.

In summary the charged  $\kappa$  is observed in the PWA analysis of the  $K_S \pi^\pm$  system recoiling against  $K^*(892)^\mp$  in the decay,  $J/\psi \rightarrow K^*(892)^\mp K_S \pi^\pm \rightarrow K_S K_S \pi^+ \pi^-$ . The  $K_S K_S \pi^+ \pi^-$  data are selected from six charged track events of the 58 million  $J/\psi$  decays obtained by BESII at BEPC. Contributions from backgrounds in the selections of the  $K_S K_S \pi^+ \pi^-$  events and of the  $K^*(892)^\mp K_S \pi^\pm$  events are considered. The partial wave analysis is performed based on the VMW method, and  $\chi^2$  fitting is utilized for the fit. Breit-Wigner parameters for the charged  $\kappa$  resonance are obtained in the analysis. The mass and width parameters of the resonances contributing the process except the charged  $\kappa$  are fixed in the analysis to those of the PDG tables. Their uncertainties and those from the estimation of the backgrounds are included in the estimation of the systematic errors for the charged  $\kappa$  parameters. The parameters of the charged  $\kappa$  are in agreement with those for the neutral  $\kappa$ . The branching ratio of charged  $\kappa$  of the decay,  $J/\psi \rightarrow K^*(892)^\mp \kappa^\pm$  is obtained. The result is consistent with that obtained recently at BESII for the charged  $\kappa$  in the different channels of the  $J/\psi$  decays.

## Acknowledgments

The BES Collaboration thanks the staff of BEPC and computing center for their hard efforts. This work is supported in part by the National Natural Science Foundation of China under contracts Nos. 10491300, 10225524, 10225525, 10425523, 10625524, 10521003, 10821063, 10825524, the Chinese Academy of Sciences under contract No. KJ 95T-03, the 100 Talents Program of CAS under Contract Nos. U-11, U-24, U-25, and the Knowledge Innovation Project of CAS under Contract Nos. U-602, U-34 (IHEP), the National Natural Science Foundation of China under Contract Nos. 10775077, 10225522 (Tsinghua University), the Core University Program of Japan Society for Promotion of Science, JSPS under contract No. JR-02-B4 (KEK and Universities), the fund for the international collaboration and exchange (Nihon-U), Grants-in-Aid for Science Research under contract No. C18540281 (U. Miyazaki), and the Department of Energy under Contract No. DE-FG02-04ER41291 (U. Hawaii).

## References

- [1] C. Amsler et al, Particle Data Group, Phys. Lett. **B567** (2008) 1.
- [2] E. van Beveren et al., Z. Phys. **C30** (1986) 615.
- [3] S. Ishida et al., Prog. Theor. Phys. **98** (1997) 621.

- [4] D. Black et al., Phys. Rev. **D58**, (1998) 054012.
- [5] J.A. Oller and E. Osset, Phys. Rev. **D60** (1999) 074023.
- [6] M.J. Jamin et al., Nucl. Phys. **B587** (2000) 331.
- [7] D. Bugg, Phys. Rev. Lett. **B572** (2003) 1.
- [8] J.R. Pelaez, Mod. Phys. Lett. **A19** (2004) 2879.
- [9] H.Q. Zheng et al., Nucl. Phys. **A733** (2004) 235.
- [10] Z.Y. Zhou and H.Q. Zheng, Nucl. Phys. **A775** (2006) 212.
- [11] S. Descotes-Genon and B. Moussallam, Eur. Phys. J. **C48** (2006) 553.
- [12] F.K. Guo et al., Nucl. Phys. **A773** (2006) 78.
- [13] E.M. Aitala et al. (Fermilab E791 Collaboration), Phys. Rev. Lett. **89** (2002) 121801.
- [14] M. Ablikim et al. (BES Collaboration), Phys. Lett. **B633** (2006) 681.
- [15] J.M. Link et al. (FOCUS Collaboration), Phys. Lett. **B535** (2002) 43.
- [16] J.M. Link et al. (FOCUS Collaboration), Phys. Lett. **B653** (2007) 1.
- [17] J.M. Link et al. (FOCUS Collaboration), Phys. Lett. **B681** (2009) 14.
- [18] G. Bonvicini et al. (CLEO Collaboration), Phys. Rev. **D78** (2008) 052001.
- [19] C. Cawlfeld et al. (CLEO Collaboration), Phys. Rev. **D74** (2006) 031108.
- [20] D. Epifanov et al. (Belle Collaboration), Phys. Lett. **B654** (2007) 65.
- [21] S. Paramesvaran (BaBar Collaboration), Proc. of the DPF-2009 Conf. Detroit, MI. 2009; arXiv0910.2884[hep-ex].
- [22] B. Aubert et al. (BaBar Collaboration), Phys. Rev. **D76** (2007) 011102.
- [23] M. Ablikim et al. (BES collaboration), Phys. Lett. **B693** (2010) 88.
- [24] J.Z. Bai et al. (BES collaboration), Nucl. Instr. Methods, **A344** (1994) 319; J.Z. Bai et al. (BES collaboration), Nucl. Instr. Methods, **A458** (2001) 627.
- [25] S. Ishida et al., Prog. Theor. Phys. **95** (1996) 745; M. Ishida et al., Proceedings of International Symposium on Hadron Spectroscopy, Chiral Symmetry and Relativistic Description of Bound Systems, Tokyo, 24-26February, 2003, in: KEK Proceedings **2003-7** 2003, p. 143, hep-ph/0308308.
- [26] T. Komada, Proceedings of 10th Hadron Spectroscopy Conference, Aschaffenburg, Germany, 31 August - 6 September, 2003, AIP Conf. Proc. **717** (2004) 337.
- [27] M. Ablikim et al. (BES collaboration), Nucl. Instr. Methods **A552** (2005) 344.
- [28] F. James, "MINUIT, Function Minimization and Error Analysis, version 94.1" Report No. CERN D506 (1994) (unpublished).